

Burn Scar Delineation from Landsat Imagery Using Modified Chan-Vese Model

SHEN Chaomin

Joint Laboratory for Imaging Science & Technology, *and* Dept of Computer Science
East China Normal University
Shanghai 200062, P.R. China
cmshen@cs.ecnu.edu.cn

PI Ling

Dept of Mathematics, East China Normal University
Shanghai 200062, P.R. China
plingzh@eyou.com

LI Fang

Dept of Mathematics, East China Normal University
Shanghai 200062, P.R. China
lifang@eyou.com

FAN Jinsong

School of Mathematics and Information Science, Wenzhou University,
Wenzhou, Zhejiang Province 325000, P.R. China
and
Dept of Mathematics, East China Normal University
Shanghai 200062, P.R. China
fjs@wzu.edu.cn

Abstract: In this paper, we propose a novel semi-automatic method for burn scar delineation from Landsat imagery using modified Chan-Vese model. Burn scars show reddish-brown from Landsat's band 742 combination. This feature can be used for semi-automatic delineation of burn scars. Usual segmentation algorithms detect all objects in the image, while our goal is to detect burn scars from a given Landsat image, regardless of other objects. Our algorithm is based on segmenting objects of interest (OOI) using modified Chan-Vese model. Firstly, we choose sample pixels visually from the burn scar. From these sample pixels, a discrimination function for whether a pixel belongs to burn scar or not is determined by the principal component analysis and interval estimation. Then we define a modified Chan-Vese functional. In order to minimize this modified Chan-Vese functional, the evolution equation corresponding to the functional is given. The initial contour of the evolution is a function of the discrimination function, and automatically located near the boundary of OOI. An improved stopping function is used in our evolution equation. Our stopping function depends on image gradient and the discrimination function. This stopping function helps the evolving curve reaches the exterior and interior boundaries of burn scar fast and accurately. Landsat imagery of burn scars over Russia is used to test our algorithm. The result shows that the algorithm is very accurate for delineating exterior and interior burn scar boundaries.

Keywords: burn scar, Landsat, Chan-Vese model, objects of interest.

1. Introduction

Forest fires occur in various parts of the world every year. Forest fires and resultant burn scars can be observed in satellite images. In order to evaluate fire situation and the damage of fire, delineation of burn scars from satellite images is often a routine work [1].

In order to delineate burn scars, we first should know the feature of burn scars in satellite images. Given a satellite image, if some physical quantities such as radiance, reflectance, and NDVI are known, it would be helpful to distinguish burn scars from other objects. But, in many cases, the only resource available is a color image with fires or burn scars in it. Burn scars can still easily be distinguished by visual inspection if we really know what they look like [2]. In this paper,

we discuss the delineation of burn scars from Landsat images with combination of Band 742, i.e., Band 7, 4 and 2 is shown in Red, Green, and Blue respectively.

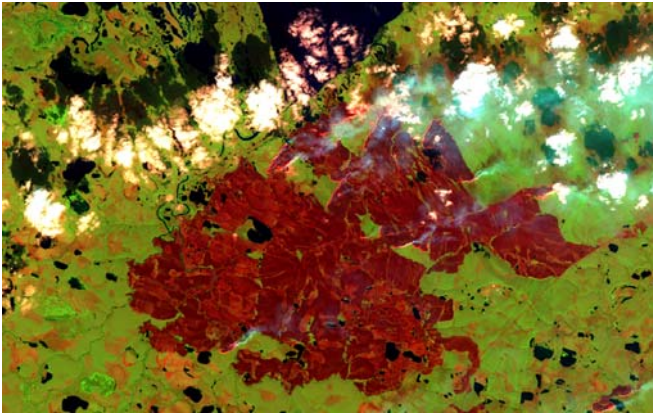


Fig. 1 Image showing burn scar (approximately 18km ×11km), acquired on 2002-08-16 over Chukotka, Russia

Delineation of burn scar by hand is a tedious work, and the delineation is not quite accurate since it is very difficult to exactly follow the burn scar boundary by mouse click. Burn scars show reddish-brown from Landsat's Band 742 combination, and this feature can be used for semi-automatic or automatic delineation of burn scars. For example, an ESA backed, Earth observation based service used Landsat images to automatically detect the 2004 burn scars within some fire-prone areas in Europe [3].

In this paper, we propose a novel semi-automatic method for burn scar delineation using modified Chan-Vese model.

The study area is Chukotka, Russia. Figure 1 shows the image with burn scars.

Section 2 describes how to delineate burn scars in Landsat images. Section 2.1 discusses general geodesic active models and why they are not applicable to our case. Section 2.2 describes our algorithm using modified Chan-Vese model. Section 3 shows the result of the delineated burn scars from the Landsat image. The result is also analyzed in this section. Section 4 concludes the paper.

2. Burn scar delineation using geodesic active contour method and Chan-Vese model

Our aim is to delineate burn scars from Landsat images such as Figure 1. The Landsat image is from Global Land Cover Facility (GLCF), University of Maryland (Courtesy of U.S. Geological Survey) [4]. Figure 1 has been acquired on 2002-08-16 over Chukotka, Russia. The path number is 92, and the row number is 15.

We first discuss the mathematical problem of delineating burn scars in Figure 1. Mathematically, our problem is to find a solution on how to delineate the boundaries of Objects of Interest (OOI). In our case, the OOI are burn scars.

Before proposing our method, we first review common methods for boundary delineation.

Generally speaking, there are two categories of methods for delineating boundaries of objects: edge detection methods and active contour methods. Edge detection methods have two disadvantages: detected edges may be not continuous and may contain many un-wanted points. So edge detection is not suitable for our case. Therefore, we adapt active contour methods.

2.1 From the snake algorithm, the level set method to Chan-Vese model

Active contour methods do not have the disadvantages mentioned in edge detection methods. But existing active contour methods can not be directly used to our burn scar delineation problem and thus we will propose our algorithm in Section 2.2.

The first active contour method was the snake algorithm [5]. The main idea of the snake algorithm is as follows: Given an initial contour in an image, we can define a corresponding energy. If the contour changes, the energy will change accordingly. When the energy reaches its minimum, the corresponding contour is regarded as the boundary of object(s). The contour evolves like a snake, and thus the algorithm gets its name.

Regarding our case, the snake algorithm has two problems: the first problem is that it cannot handle changes in topology. For example, if the initial contour is a circle, no matter how to evolve, it can not evolve to two circles. Thus, the snake algorithm is only applicable to detecting the boundaries of objects that with the same topology as the initial contour. The

topology of burn scars may be very complicated in some cases. For example, we have no prior knowledge of the number of burn scars in the image before the delineation is conducted. Even for one piece of burn scar, we may also encounter complicated structures such as the shape of burn scar is like a donut with center unburnt. Thus, for a given initial contour, we can not assume the topology of burn scars is the same as the initial contour. The other problem is that the snake algorithm can not detect interior boundaries (if the burn scars have any). If we give an initial contour, say, the boundary of the image, and let it shrink, when it reaches the exterior boundary, it will terminate evolution. For these two reasons, the snake algorithm is not applicable to burn scar delineation.

The level set method is an improved contour evolution method due to J. Sethian and S. Osher [6]. Better than the snake algorithm, it can handle topology changes in evolution. The main idea of the level set method is to construct a family of surfaces $z = \phi(x, y, t)$, where x, y are image coordinates, t is time, such that the intersections of these surfaces and $z = 0$ are evolving contours. For a given time t , $\phi(x, y, t) = 0$ is the contour in the (x, y) plane. Thus, $\phi(x, y, 0) = 0$ represents the initial contour and $\phi(x, y, t \rightarrow \infty) = 0$ tends to the desired contour of objects. The evolving level set function $z = \phi(x, y, t)$ can be obtained by solving its corresponding partial differential equations.

But even the level set method also can not be directly applied to burn scar delineation due to two reasons. The first reason is that the evolving contour may stop at some non burn scars points. In level set theory, for every point in the image, a stopping function is defined. The stopping function indicates the speed of evolution at that point. If the value of stopping function is very big, the curve will run past that point with the speed valued by stopping function along a certain direction. If the speed is reaching 0, the curve will stop at that point. Usually, the stopping function is defined as a decreasing function of the gradient and only depends on the gradient, i.e., at the location where the gradient is big, the stopping function is small, which means evolution tends to stop at that location. So the evolution curve of level set method may stop at the place where the gradient is big, but that place may not be OOI at all. This problem can be solved if a “good” stopping function is defined. A good stopping function means that it is small if and only if two conditions are satisfied: 1) the point is in burn scar area, and 2) that point has a big gradient. In section 2.2 we will construct a stopping function of such kind.

The second reason that the level set method can not be directly used is similar to the problem mentioned for the snake algorithm: when the evolved curve meets the exterior boundary, it will terminate evolution. Assume that the initial curve is the image boundary, after several evolutions, it successfully arrives at the exterior boundary of burn scars. We want it shrink again and also find the interior boundary if the interior boundary exists. But since the stopping function reaches 0 at the exterior boundary, the curve will not march on. Thus, the interior boundary can not be detected.

The Chan-Vese model (CV model) proposed by Chan and Vese can solve this problem [7]. An energy functional is defined in the CV model. Like the snake algorithm, when the energy reaches its minimum, the corresponding contour is regarded as the boundary of object(s). The CV-derived contour can delineate exterior and interior boundaries of object(s) because of the “fitting energy” term in the functional. The original CV model only deals with delineating boundaries of all objects in the image. We shall generalize it to delineating only OOI (burn scars in our case), regardless of all other objects.

2.2 Our algorithm of delineating boundaries of burn scars

As discussed in Section 2.1, for our problem, the difficulties are in two aspects. 1) The topology of the burn scar may be complicated. For example, the burn scar may have interior and exterior boundaries. 2) Only boundaries of burn scar are wanted in the final result. Other features should be excluded.

In order to overcome these two difficulties, following problems should be solved.

1. determine the properties of burn scar pixels and give out a criterion whether a pixel is in burn scar area;
2. give the stopping function at each point in the image. The stopping function should be small if and only if the point is in burn scar and the gradient at that point is big;
3. give the evolution equation corresponding to the modified CV model;
4. give the numerical solution of the equation.

In what follows, assume the image is a color image $I(x_1, x_2)$ unless stated otherwise. Let $x = (x_1, x_2)$, the image also can be expressed by $I(x)$, where $I(x)$ is a vector denoted by $I(x) = (I_1, I_2, I_3) = (R, G, B)$.

2.2.1 Properties of burn scar pixels and interval estimation of burn scar pixels

Suppose we start evolution. During the evolution, when the curve evolves to a new point, the speed and direction at that point should be given. Outside the burn scar area, the speed should be big so that the algorithm can be efficient, and when reaching the boundary of burn scar, the speed should be approaching zero. Inside the burn scar area, the speed should also be big until interior boundary is met. So the discrimination function of whether a point is in burn area or not should be given. To construct this discrimination function, the properties of the burn scar pixels should be studied. This is done by choosing some sample points of the burn scars. Then properties of burn scar population are estimated from these samples.

Thus, we first discuss the properties of the burn scar pixels. Since the image is displayed in Red, Green, Blue (RGB for short) combination, we want to set up a criterion that describes whether a point is a burn scar point using a discrimination function of R, G, and B. For example, one simple criterion might be: "a point is regarded as a burn scar if and only if 1) $R \in [a_1, b_1]$, 2) $G \in [a_2, b_2]$, and 3) $B \in [a_3, b_3]$, where $a_i, b_i, i=1, 2, 3$ are some integers". We want the criterion as precise as possible, i.e., should avoid "type I error" (omission) and "type II error" (commission).

It is quite intuitive that the above mentioned rectangular parallelepiped may not best describe the burn scar situation. Before the burn scar study is done, the distribution of burn scar points may have any shape to us. For example they may concentrate along certain line in RGB co-ordinates. If so, using a rectangular parallelepiped criterion in RGB co-ordinates will definitely cause type II error, which could be avoided by using rectangular parallelepiped criterion in a new co-ordinate system with the concentration line as the new X-axis. So we should find if there exists a co-ordinate system better than RGB system, so that in that new system the discrimination function is simple and precise. Principal Component Analysis (PCA) is a way to find out this kind of new system. For the detail of PCA, please refer to [8].

The main procedures of PCA are as follows. In $I(x_1, x_2)$, we choose n sample pixels $(x_{11}, x_{12}, x_{13}), \dots, (x_{n1}, x_{n2}, x_{n3})$ from burn scars. Therefore, $X = (x_{ij})$ is an $(n \times 3)$ matrix. Let $X^* = (x_{ij}^*)_{n \times 3}$ be the normalized matrix of X . If the correlation coefficient matrix of X^* is denoted by $\rho = (\rho_{ij})_{3 \times 3}$, then the corresponding eigenvectors of ρ are axes of the new co-ordinate system. Assume the eigenvalues are λ_1, λ_2 and λ_3 ($\lambda_1 \geq \lambda_2 \geq \lambda_3$). Corresponding eigenvectors are $\omega_1, \omega_2, \omega_3$, where ω_i ($i=1,2,3$) is a column. Then a point (x_{i1}, x_{i2}, x_{i3}) in the RGB co-ordinate system can be written as (p_{i1}, p_{i2}, p_{i3}) in the new co-ordinate system, i.e., if let $P = (p_{ij})_{n \times 3}$, then $P = X(\omega_1, \omega_2, \omega_3)$. If a vector is denoted by $a = (a_1, a_2, a_3)$ in the new co-ordinate system, then a_i is called the i -th principal component of a ($i=1,2,3$). The

percentage of contribution of the i -th principal component to the total sample variance is $e_i = \frac{\lambda_i}{\lambda_1 + \lambda_2 + \lambda_3}, i=1, 2, 3$

which measures the importance of the i -th principal component. If the percentage of contribution of the first principal component, e_1 , is big enough, the information from R, G, B can be mostly explained by the first principal component. Thus, only the first principal component is needed to be considered. In what follows, we construct an interval in ω_1 axis by the method of interval estimation. The interval should cover almost all n samples by interval estimation.

Letting $\bar{P}_1 = \frac{1}{n} \sum_{i=1}^n p_{i1}, S_{P_1} = \sqrt{\frac{1}{n-1} \sum_{i=1}^n (p_{i1} - \bar{P}_1)^2}$, we can use t -distribution with $n-1$ degrees of freedom to construct

a confidence interval $\left[\bar{P}_1 - \frac{S_{P_1}}{\sqrt{n}} \cdot t_{\frac{\alpha}{2}}, \bar{P}_1 + \frac{S_{P_1}}{\sqrt{n}} \cdot t_{\frac{\alpha}{2}} \right]$ with degree of confidence $1-\alpha$, where $t_{\frac{\alpha}{2}}$ is the t -value with $n-1$ degrees of freedom and $0 < \alpha < 1$, usually $\alpha = 0.05$ (i.e., 95% confidence).

The above procedures can be summarized as: Every pixel in the image is transformed from RGB co-ordinates to the new co-ordinates via PCA. The first component in the new co-ordinates is called first principal component and contains most important information. If the value of first principal component is within the confidence interval, we regard that the pixel is in the burn scar area with a confidence of $1 - \alpha$.

Thus for a given pixel x , we could define a function $\gamma(I(x))$, which describes whether this point is in burn scar area or not. Supposing that the confidence interval obtained by PCA is $[a, b]$, and the value of first principal component is $\tilde{u}(I(x))$, then $\gamma(I(x))$ is defined by

$$\gamma(I(x)) = \begin{cases} 1 & a \leq \tilde{u}(I(x)) \leq b, \\ 0 & \text{others.} \end{cases}$$

This information is used in the construction of stopping function below.

2.2.2 Stopping function

We shall now define our stopping function.

A stopping function is a decreasing function of gradient. Usually, it only depends on gradient, regardless of other image information. For example, for a grey image $I(x)$,

$$g(x) = \frac{1}{1 + \frac{|\nabla(G_\sigma * I)|^2}{K^2}}$$

is a typical stopping function, where $K > 0$ is a contrast factor, $G_\sigma(x) = \sigma^{-\frac{1}{2}} \frac{1}{2} \exp\left(-\frac{|x|^2}{4\sigma}\right)$ is a Gaussian filter with a

parameter σ , ∇ is the gradient operator, and $*$ is the convolution operator.

This kind of stopping function has disadvantages mentioned in 2.1 and it is only for grey images. We want to define a new stopping function for color images. A good stopping function should be small if and only if two conditions are satisfied: 1) the point is in burn scar area, and 2) that point has a big gradient.

In color images, the concept of gradient is the largest eigenvalue Λ of the following matrix:

$$\begin{pmatrix} 1 + R_{x_1}^2 + G_{x_1}^2 + B_{x_1}^2 & R_{x_1} R_{x_2} + G_{x_1} G_{x_2} + B_{x_1} B_{x_2} \\ R_{x_1} R_{x_2} + G_{x_1} G_{x_2} + B_{x_1} B_{x_2} & 1 + R_{x_2}^2 + G_{x_2}^2 + B_{x_2}^2 \end{pmatrix},$$

where R, G and B represents the pixel's value of red, green and blue after Gaussian convolution respectively; $R_{x_1} = \partial_{x_1} R, \dots$. For the detailed definition of Λ , please refer to [9, 10].

Our stopping function is

$$g(x) = \frac{1}{1 + (G_\sigma * \gamma) \Lambda^2}. \quad (1)$$

It can be verified that (1) satisfies the two conditions mentioned.

2.2.3 Modified CV model and evolution equation

Assume that in a grey image $I(x_1, x_2)$, the region enclosed by \mathcal{C} is denoted by ϖ . The whole image domain is denoted by Ω . Then, the original CV energy function is:

$$\begin{aligned} E(c^+, c^-, \mathcal{C}) &= \mu \cdot \text{Length}(\mathcal{C}) + \nu \cdot \text{Area}(\text{inside}(\mathcal{C})) \\ &+ \lambda^+ \int_{\text{inside}(\mathcal{C})} |I(x_1, x_2) - c^+|^2 dx_1 dx_2 + \lambda^- \int_{\text{outside}(\mathcal{C})} |I(x_1, x_2) - c^-|^2 dx_1 dx_2, \end{aligned} \quad (2)$$

where $\mu \geq 0, \nu \geq 0, \lambda^+, \lambda^- > 0$ are fixed parameters; and c^+, c^- are two constants to be determined; The first two terms are regularizing terms, and last two terms are ‘‘fitting energy’’ which is used to control the interior and exterior boundaries.

Then, the CV model is to find the minimization of (2), i.e., find $\{c^+, c^-, \mathcal{C}\}$ such that

$$\min_{c^+, c^-, \mathcal{C}} E(c^+, c^-, \mathcal{C})$$

is reached.

We now generalize the energy of (2) into color images, and we use the notations of the level set function ϕ (ref. [6]). Recall that $\phi = 0$ is an implicit representation of \mathcal{C} , i.e., $\mathcal{C} = \{(x_1, x_2) : \phi(x_1, x_2, t) = 0\}$ is the contour at evolution time t in the color image.

Our modified CV functional is defined by

$$\begin{aligned} E(\phi, \mathcal{C}^+(\phi), \mathcal{C}^-(\phi)) &= \frac{\eta}{2} \int_{\Omega} (|\nabla \phi| - 1)^2 dx_1 dx_2 + \mu \int_{\Omega} g |\nabla H_{\varepsilon}(\phi)| dx_1 dx_2 + \nu \int_{\Omega} g \cdot H_{\varepsilon}(\phi) dx_1 dx_2 \\ &+ \frac{1}{3} \int_{\text{inside}(\mathcal{C})} (G_{\sigma} * \gamma) \sum_{i=1}^3 \lambda_i^+ |I_i(x_1, x_2) - c_i^+|^2 H_{\varepsilon}(\phi) dx_1 dx_2 \\ &+ \frac{1}{3} \int_{\text{outside}(\mathcal{C})} (G_{\sigma} * \gamma) \sum_{i=1}^3 \lambda_i^- |I_i(x_1, x_2) - c_i^-|^2 (1 - H_{\varepsilon}(\phi)) dx_1 dx_2 \end{aligned} \quad (3)$$

where $\phi, \mu, \nu, g(x), G_{\sigma}, \gamma, I_i$ are as defined before; $\lambda_i^-, \lambda_i^+, c_i^-, c_i^+$ are the generalizations of $\lambda^+, \lambda^- > 0, c^-, c^+$ in color images; η is a constant called penalty constant; $H_{\varepsilon}(\phi)$ is the regularization of Heaviside function,

$$H_{\varepsilon}(\phi) = \frac{1}{2} \left(1 + \frac{2}{\pi} \arctan \left(\frac{\phi}{\varepsilon} \right) \right).$$

Comparing (2) and (3), the first term in (3) is a new term. This term is called penalizing term. It measures the deviation of level set function ϕ from signed distance function (ref. [11]).

The second and the third term in (3) are the generalizations of the first and the second term of (2). In (3), these two terms are used so as to the contour will stop at the places where the stopping functions are small.

The corresponding minimization problem is

$$\min_{\phi, \mathcal{C}^+, \mathcal{C}^-, \mathcal{C}} E(\phi, \mathcal{C}^+(\phi), \mathcal{C}^-(\phi)) \quad (4)$$

For the detail of mathematical description of our algorithm, please refer to [12].

2.2.4 Numerical solution of modified CV model

In order to find the solution of (4), we compute the first variation of $E(\phi, \mathcal{C}^+(\phi), \mathcal{C}^-(\phi))$ respective to ϕ, \mathcal{C}^+ , and \mathcal{C}^- , and get the corresponding Euler-Lagrange equations. We also use the method of negative gradient flow to the Euler-Lagrange equation respective to ϕ . Then, we have

$$c_i^+(\phi) = \frac{\int_{\Omega} I_i(x_1, x_2) H_{\varepsilon}(\phi(x_1, x_2)) dx_1 dx_2}{\int_{\Omega} H_{\varepsilon}(\phi(x_1, x_2)) dx_1 dx_2}, \quad c_i^-(\phi) = \frac{\int_{\Omega} I_i(x_1, x_2) (1 - H_{\varepsilon}(\phi(x_1, x_2))) dx_1 dx_2}{\int_{\Omega} (1 - H_{\varepsilon}(\phi(x_1, x_2))) dx_1 dx_2} \quad (5)$$

$$\frac{\partial \phi}{\partial t} = \eta \operatorname{div} \left[\left(1 - \frac{1}{|\nabla \phi|} \right) \nabla \phi \right] + \delta_{\varepsilon}(\phi) \left[\mu \operatorname{div} \left(g \frac{\nabla \phi}{|\nabla \phi|} \right) - \nu \cdot g - \frac{G_{\sigma} * \gamma}{3} \sum_{i=1}^3 \lambda_i^+ (I_i - c_i^+)^2 + \frac{G_{\sigma} * \gamma}{3} \sum_{i=1}^3 \lambda_i^- (I_i - c_i^-)^2 \right] \quad (6)$$

$$\phi(x_1, x_2, 0) = \phi_0(x_1, x_2), \quad \text{in } \Omega$$

$$\frac{\delta_{\varepsilon}(\phi)}{|\nabla \phi|} \frac{\partial \phi}{\partial n} = 0, \quad \text{on } \partial \Omega$$

where $\delta_{\varepsilon}(\phi)$ is the derivative of $H_{\varepsilon}(\phi)$ (Ref. [13]); the initial $\phi_0(x_1, x_2)$ is given by

$$\phi_0(x_1, x_2) = \rho \cdot \left(G_{\sigma} * \gamma(I(x_1, x_2)) - \frac{1}{2} \right),$$

where $\rho > 0$ is a constant suggested to be larger than 2ε . Recall that $\phi_0(x_1, x_2) = 0$ is the initial contour. From the definition of γ and the expression of $\phi_0(x_1, x_2)$, it is easy to see if γ is absolutely accurate, $\phi_0(x_1, x_2) = 0$ is already the interior and exterior boundaries of the OOI. But this discrimination of whether a point is a burn scar point may have type I error or type II error. Thus $\phi_0(x_1, x_2) = 0$ may be not the exact boundaries of the OOI yet, but $\phi_0(x_1, x_2) = 0$ is quite close to the real boundaries already.

The iteration formula of ϕ in (6) is

$$\phi_{x_1, x_2}^{n+1} = \phi_{x_1, x_2}^n + \tau \cdot L(\phi_{x_1, x_2}^n), \quad (7)$$

where τ is the time step, and L is the right hand side of (6). Here (x_1, x_2) is the grid points and n means the n -th iteration.

We can make a short summary of what we have done in our algorithm:

1. choose sample pixels from burn scars;
2. start evolution; The initial ϕ^n ($n = 0$) is defined by ϕ_0 ;
3. during the evolution, compute $c_i^+(\phi^n)$ and $c_i^-(\phi^n)$ ($i = 1, 2, 3$) using (5); compute ϕ^{n+1} using (7);

When $\phi(x_1, x_2)$ is given, the next step is to find the level set $\phi(x_1, x_2) = 0$, i.e., the solutions $\{(x_1, x_2)\}$ such that $\phi(x_1, x_2) = 0$.

The exact solutions $\{(x_1, x_2)\}$ of $\phi(x_1, x_2) = 0$ should be real numbers. But, because of the discreteness of grid points, we need to find the integer solutions of $\phi(x_1, x_2) = 0$. Finding the integer solutions of $\phi(x_1, x_2) = 0$ can be done by

comparing every pixel (x_1, x_2) with its 8-neighborhood pixels. If we define $\operatorname{sign}(x_1, x_2) = \begin{cases} 1 & \text{if } \phi(x_1, x_2) \geq 0 \\ -1 & \text{else.} \end{cases}$, then

(x_1, x_2) is regarded as the solution of $\phi(x_1, x_2) = 0$ if and only if

$$8 \cdot \operatorname{sign}(x_1, x_2) - \sum_{(y_1, y_2) \in 8\text{-neighbor of } (x_1, x_2)} \operatorname{sign}(y_1, y_2) \geq 0,$$

i.e., the sign of $\phi(x_1, x_2)$ changes in the 8-neighborhood of (x_1, x_2) .

Thus, the contour $\phi(x_1, x_2) = 0$ is found.

3. Results

Figure 2 shows the result of delineation of interior and exterior boundaries of burn scar.

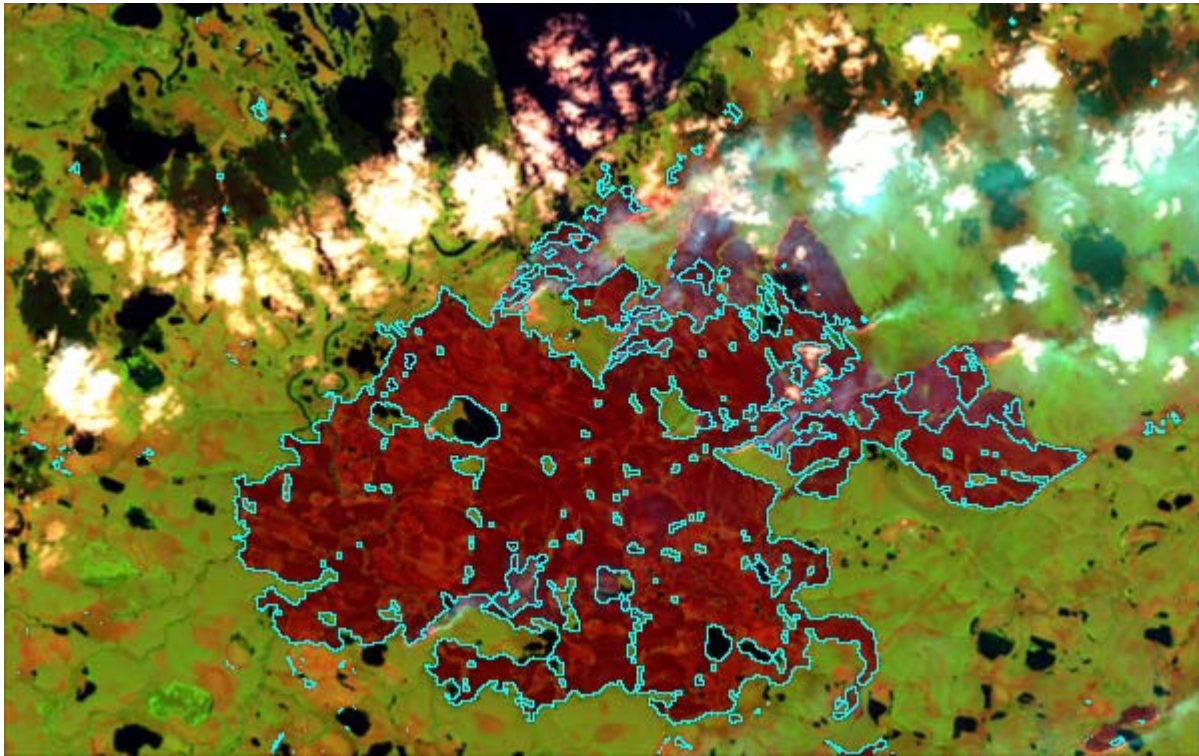


Fig. 2 Result of burn scar delineation

In general, the result is quite promising. In the image, there are one big burn scar with complicated topological structure and several small burn scars scattered around. The delineation results of both big and small burn scars are satisfactory.

For the big burn scar, the real exterior boundaries are almost delineated, except for some missing areas, especially in burning areas with smokes. The real interior boundaries are also almost delineated, while there are some tiny delineated boundaries may be not quite necessary. But most of those “unnecessary” interior boundaries should not be considered as wrong. The areas inside and outside the boundaries still look different, although not quite obvious. Those “tiny” boundaries could be removed if some constraints such as minimum perimeter are added to the algorithm

For the small burn scars, most of them are delineated. Some delineated burn scars are smaller than their real shape, i.e., the contour over shrink, especially in the burning area with smokes. This can be improved slightly if the selection of sample pixels from burn scars is done precisely.

One problem of our algorithm is that this algorithm tends to miss some burning areas if we do not want non burn scars also delineated, although different selections of sample points will cause different results. The reason is that the property of pixels in those burning areas of burn scar is slightly from other burn scar pixels, i.e., the OOI is not so uniform. Thus the discrimination function based on only one interval obtained by using interval estimation only once may be not accurate enough.

This can be improved by regarding the whole non-uniform OOI as the combination of several small OOIs. Each of small OOI is almost uniform. For each small OOI, we can have a discrimination function. Then we can get the discrimination function of the whole OOI by combining the discrimination functions of small OOIs.

4. Conclusion

Forest fires and resultant burn scars can be observed in Landsat images. Burn scars show reddish-brown from Landsat's band 742 combination. This feature can be used for semi-automatic delineation of burn scars. In this paper, we have proposed a novel semi-automatic method for burn scar delineation from Landsat imagery using modified Chan-Vese model. This method can detect interior and exterior boundaries of burn scars.

Landsat imagery of burn scars over Russia is used to test our algorithm. We have constructed one discrimination function of burn scar based on the sample points choosing from burn scar areas. Then we define a modified Chan-Vese functional and find the solution to the minimization of this functional. The solution curve is the interior and exterior boundaries of burn scars. The result is satisfactory. Most of burn scars are accurately delineated.

The delineation result could be improved by constructing a more accurate discrimination function of burn scars. The whole burn scar areas can be viewed the combination of burning burn scars and unburning burn scars. The whole burn scars may be not uniform, but each small category can be regarded as uniform. For each uniform part, we can have a discrimination function respectively. Then we can get the discrimination function of the whole burn scars by combining the discrimination functions of burning and unburning burn scars together.

This modified Chan-Vese model is applicable to delineating the interior and exterior boundaries of OOI, especially those OOIs with uniform structures.

Acknowledgement

The authors would like to thank Global Land Cover Facility (GLCF), University of Maryland for providing the Landsat imagery. The first author would also like to thank the Centre for Remote Imaging, Sensing and Processing (CRISP), National University of Singapore where he acquired basic knowledge about delineating burn scars in satellite images.

References

- [1] Shen, C.M., Liew, S.C., and Kwoh, L.K., 2001. Spatial and temporal pattern of forest/plantation fires in Riau Province, Sumatra from 1998 to 2000, *Proc. of the 22nd Asian Conference on Remote Sensing*, 5-9 November 2001, Singapore, vol. 1, 520-525.
- [2] Liew, S.C., Lim, O.K., Kwoh, L.K., and Lim, H., 1998. Study of the 1997 forest fires in South East Asia using SPOT quicklook mosaics. *Proc. of 1998 International Geoscience and Remote Sensing Symposium*, vol. 2, 879-881.
- [3] **URL:** Satellites are tracing Europe's forest fire scars. http://www.esa.int/esaEO/SEMNMV4QWD_index_0.html
- [4] **URL:** Global Land Cover Facility Homepage. Available at: <http://glcf.umiacs.umd.edu/index.shtml>
- [5] Kass, M., Witkin, A., and Terzopoulos, D., 1988. Snakes: Active contour models, *International Journal of Computer Vision*, vol. 1, 321-331.
- [6] Osher, S., Sethian, J.A., 1988. Fronts propagating with curvature-dependent speed: Algorithms based on Hamilton—Jacobi formulations, *Journal of Computational Physics*, 79, 12-49.
- [7] Chan, T., Vese, L., 2001. Active contour without edges for vector-valued image, *Journal of Visual Communication and Image Representation*, vol. 11, 130-141.
- [8] Anderson, T. W., 1984. *An introduction to multivariate statistical analysis (2nd Edition)*, Wiley, New York.
- [9] Sochen, N., Kimmel, R., and Malladi, R., 1988. A general framework for low level vision, *IEEE Trans. Image Processing*, vol. 7, 310-318.
- [10] Goldenberg, R., Kimmel, R., Rivlin, E., and Rudzsky, M., 2001. Fast geodesic active contours, *IEEE Trans. Image Processing*, vol. 10, 1467-1475.
- [11] Li, C.M., Xu, C.Y., Gui, C.F., and Fox, M.D., 2005. Level set evolution without re-initialization: a new variational formulation, *IEEE International Conference on Computer Vision and Pattern Recognition (CVPR)*, 430-436.
- [12] Pi, L., Shen, C.M., and Li, F., 2005. A new variational formulation for segmenting desired objects in color images, *preprint*.
- [13] Zhao, H.-K., Chan, T., Merriman, B., and Osher, S., 1996. A variational level set approach to multiphase motion, *J. Comp. Phys.*, vol. 127, 179-195.